Submission No.: 94

"Experimental Investigation on Concentric tube Heat Exchanger with Perforated Disk inserts using MWCNT-Water based Nanofluid"

Krishnamurthy K. N[1]., Akashdeep B. N[2]., G. F. Ali Ahammed[3], Ganesha T[1].

[1]Department of Mechanical Engineering, Visvesvaraya Technological University, Centre for Post Graduate Studies, Mysuru 570029 Karnataka, India.

[2]Department of Mechanical Engineering, K.S. School of Engineering & Management, Bengaluru 560109, Karnataka, India.

[3]Department of Computer Science Engineering, Visvesvaraya Technological University, Centre for Post Graduate Studies, Mysuru 570029 Karnataka, India.

krishnamurthy@vtu.ac.in; bndeep@gmail.com; aliahammed78@gmail.com; ganeshtnaik88@gmail.com.

*Corresponding author email: krishnamurthy@vtu.ac.in

Abstract

This work examined MWCNT-water-based nanofluid in a concentric tube heat exchanger with perforated disc inserts. The concentric tube heat exchanger is fabricated with copper as inner tube (19.05 mm) and Galvanized Ironed as outer tube (50.8 mm) of length 1500 mm, perforated disk baffles were inserted in pipe and annulus. This study examines how MWCNT-water nanofluid affects heat transfer, pressure drop and thermal performance of concentric tube heat exchanger. MWCNT nanoparticles in a base fluid with Sodium Dodecyl Sulphate (SDS) as a surfactant form the nanofluid. MWCNT nanofluid with volumetric nanoparticle concentrations of 0.1, 0.125, and 0.5% by weight was tested for heat rejection and absorption (heat transfer coefficient) and compared with distilled water. Moreover, Thermo-physical properties like Density, Thermal conductivity, Dynamic viscosity, and specific heat were examined for all the concentrations. All particle concentrations had higher heat transfer coefficients than distilled water. The nanofluid at

Reynolds number 6725 with 0.1 vol% MWCNT concentration increased heat absorption by 43% and heat rejection by 53% compared to pure water. The experiment demonstrated no significant effect of pressure drop and all the experimental results obtained are in par with theoretical results.

Key Words: Heat Exchanger, MWCNT, Concentric tube, Nanofluid, Heat Transfer Coefficient.

1. Introduction

Nowadays heat exchangers are used for many applications either for cooling purpose or heating purpose. The devices that supply the flow of thermal energy from one channel (fluid) to another channel (fluid) at different temperatures are called heat exchanger. To transfer heat from hot fluid to cold fluid heat exchangers are used. It is used for heating and cooling purposes. Heat exchangers are utilised in several applications, including the oil and gas, food and chemical, air conditioning, refrigeration, dairy, automobile, space application, electronics, and power generation industries.

To optimise thermal devices, scientists are focusing more on energy utilisation. Adding nanoparticles to the base fluid is one of the best ways to optimise a thermal device. The rate of heat transfer in heat exchangers is enhanced by using a new technology known as nanofluid. Heat transfer rate in heat exchangers can be improved by utilising various Nano particles in base fluid. J. A. Eastman et al. [1] were the first to offer a new concept of an effective heat transfer fluid by immersing metallic nanoparticles in base fluids. When compared to ordinary fluids, nanofluids are projected to have great thermal conductivity. Their findings usher in a new era in nanofluid research.

A nanofluid is a compound mixture of nanoparticles in a base fluid that enhances the fluid's thermal behaviour. It is a bi-phase system compound dispersion in which the base fluid is liquid, and the nanoparticles are solid. Water, ethylene glycol, vegetable oil, transformer oil, SAE oils, and other are examples of base fluids [2]. The three types of nanoparticles are metallic nanofluids, ceramic nanofluids, and nanofluids including carbon and polymer nanotubes. Metals, metal oxides, and nanotubes are examples of nanoparticles. Metallic nanoparticles include copper (Cu), nickel (Ni), aluminium (Al), and others, while metal oxides include titanium oxide (TiO_2), aluminium oxide (Al_2O_3), copper oxide (CuO), silicon carbide (SiC), iron oxide (FeO), and others [3–6]. Other types of nanoparticles include carbon nanotubes, calcium carbonate, graphene, titanium nanotubes, and others. When compared to other micro particles, MWCNT has outstanding heat conductivity. Hybrid nanofluids are fluids that contain two types of nanoparticles floating in a base fluid. The addition of nanoparticles to conventional fluids alters the thermophysical properties of the base fluid. The hybrid nanofluids have new properties since they are made of two or more nanoparticles in the base fluid [7]. Current research indicates that using hybrid-nanofluids alternatively to mono-nanofluids can enhance the thermo-physical characteristics and performance of heat transfer devices [8–11]. In the long run, the stability of nanofluids has a significant impact on this improvement. The addition of surfactants, ultrasonication, and changes in the pH of the conventional fluid will influence the stability of the nanofluid [12–17]. In the last two decades, the use of nanofluids has been proposed to overcome constraints to improving the capacity of bigger heat exchangers. When compared to conventional heat exchangers, the inserting fluid turbulators heat exchanger has various advantages, including higher corrosion resistance, more turbulence in the flow, a smaller area requirement, and less silt. Using various nanofluids in different base-fluids increases the thermal performance of inserting fluid turbulators heat exchangers, according to research published in the past decade [18–29]. However, only a few investigations on the utilisation of hybrid nanofluids in perforated disk HE has been conducted [30–34].

Surfactants are substances that diminish the surface tension of a liquid, which is important in the distribution of one phase of the liquid over another. Surfactants are employed in base fluids to stabilise and prevent nanoparticle aggregation. When it is employed to stabilise solid particles in a base liquid, it is sometimes referred to as a dispersion. Surfactants are classified according to their head composition: non-ionic surfactants (surfactants with no charge in their heads), anionic surfactants (surfactants with negatively charged heads), cationic surfactants (surfactants with positively charged heads), and amphoteric surfactants (dispersants having zwitterionic head groups). SDS (Sodium dodecyl sulphate), SDBS (Sodium dodecyl benzene sulphate), CTAB (Cetyltrimethyl ammonium bromide), PVP (poly-vinyl-pyrrolidone), Oleic acid, acetyl trimethyl ammonium bromide, and others are examples of surfactants [8, 35, 36].

Aliakbar Karimipour et al. [37] Solids and fluids are combined to form nanofluid. In this experiment, water was used as the base fluid, and two materials, CuO and multi-walled carbon nanotubes (MWCNT), were dispersed in it. MN and HN thermal conductivity (TC) were measured at volume fractions (Vf) ranging from 0.2% to 1.0% and temperatures (T) from 25 °C to 50 °C. At the maximum Vf and T, mono-nanofluid and hybrid-nanofluid thermal conductivity gains of 19.16% and 37.05% were observed, respectively. Masoud Zadkhast et al. [38] Nanofluid is created by combining fluids and solids. In this experiment, multi-walled carbon nanotubes (MWCNT) and CuO were disseminated in water, which served as the base fluid. Thermal conductivity (TC) for MN and HN was tested at temperatures (T) ranging from 25 °C to 50 °C and volume fractions (Vf) ranging from 0.2% to 1.0%. Mono-nanofluid and hybrid-nanofluid thermal conductivity increases of 19.16% and 37.05%, respectively, were noted at the highest Vf and T. The highest thermal enhancement percentage was observed as 30.38% at T = 50℃ and Ø =0.6%.

Jian Qu et al., [39] Experimental research was done on the photothermal conversion abilities of a HyNF combination of CuO-MWCNT and H_2O nanofluids for direct solar thermal energy harvesting. To analyse and compare the optical absorption properties and photo-thermal conversion efficiency of hybrid CuO-MWCNT/H_2O nanofluids at various concentration mixing ratios (CMRs), their solar thermal energy harvesting potential was determined. With a CuO/MWCNT concentration mixing ratio of 0.15 wt%/0.005 wt%, a maximum terminal temperature rises of 14.1 °C was attained after 45 minutes of light irradiation. According to this study, hybrid CuO-MWCNT/H_2O nanofluids with acceptable CMRs might be a good alternative for directly harvesting solar thermal energy.

Iman Fazeli et al. [40] Using response surface methods, researchers evaluated the heat transmission and flow of a MWCNT-CuO hybrid nanofluid in a brazed plate heat exchanger. In 0.1 wt% of hybrid nanofluid, the stability of a mixture of two surfactants, including GA and Tween-80, was found to be satisfactory, and no sedimentation was seen. Additionally, when the hot fluid is maintained at a constant temperature of 35°C and a volume flow rate of 6 L/min, the maximum increases in the convective heat transfer coefficient of hybrid nanofluid over water at volume flow rates of 14.4, 18.9, and 24.4 L/min are 85.56%, 101.25%, and 139.19%, respectively. According to this article, GA and Tween-80 are appropriate surfactants. It also discovered improved thermal conductivity at 35°C and 6 L/min hot fluid flow rate.

In the current study, MWCNT-CuO/DI hybrid nanofluids were used in double-pipe heat exchangers with and without perforated disc inserts at volume fractions of 0.1%, 0.2%, 0.3%, and 0.4%, respectively. Two surfactants, SDS and Triton X-100, were used in an equal ratio to increase the stability of hybrid nanofluid. At different volume fractions, thermal conductivity, specific heat, density, viscosity, Reynolds number, Nusselt number, heat transfer coefficient, friction factor, pressure drop, and thermal performance factor were evaluated.

2. Experimental investigation

2.1 Preparation of MWCNT/CuO DI water hybrid nanofluid

Obtaining uniform and stable solutions is one of the key challenges in nanofluid production. A two-step approach is used in this research project to create stable hybrid nanofluid samples. This procedure involved dispersing dry multiwalled carbon nanotubes (MWCNT) and copper oxide (CuO) in distilled water at various volume concentrations of 0.1%, 0.2%, 0.3%, and 0.4%, as shown in Fig. 1. The right volume concentration of surfactants is required for the best distribution of nanoparticles into the base fluids to achieve a good dispersion. For the creation of the hybrid nanofluid in this study, DI water was used as the base fluid. Additionally, the base fluid added with equal amounts of SDS and Triton-X 100 as surfactants in the ratio (1:1) with respect to nanoparticles. As illustrated in Fig 2. after 2 hours of magnetic stirring, each sample is exposed for 8 hours to an ultrasonic processor with a power of 400 W and a frequency of 24 kHz to achieve a proper dispersion of surfactants and nanoparticles in the base fluid to obtain hybrid nanofluid. To decrease the fluid pressure point, this apparatus creates supersonic mechanical vibrations creating a higher molecular velocity. When the pressure falls below the vapour pressure, the fluid evaporates. The bubbles are then blown up by the surrounding pressure, breaking the agglomeration between the particles and forming a homogeneous stable suspension. To ensure the stability of the created nanofluid, the density fluctuation of the nanofluid with time can be used as a criterion of stability. So, over a two-week period, the density of nanofluid was measured five times (in 1st, 2nd, 5th, 8th, and 14th days). A minor change in nanofluid density was not detected while using this method. All samples are stable, and no sedimentation was reported in the longer duration prior to the experiments.

The non-ionic surfactants Triton X-100 and ionic surfactants SDS were used in this study, is purchased from Raghu chemicals Mysore. The CuO and MWCNT nanoparticles were purchased from Ultra Nanotech Pvt., Ltd., Bengaluru. As demonstrated in Fig. 3 and 4, the structural characteristics and morphology of MWCNT and copper oxide nanoparticles are studied using X-ray diffraction (XRD), Scanning Electron Microscope (SEM), and Transmission Electron Microscope (TEM) respectively. The average size of nanoparticles is obtained by using an XRD image (Bruker-D8 Germany) and the Debye-Scherrer equation $d = 0.89\lambda/(\beta\cos\theta)$, where d represents the particle diameter size, λ represents the X-ray wavelength (0.1541), implies the full width at half maximum, and finally, θ illustrates the Bragg's angle. Table 1. demonstrates the various values of thermophysical properties and morphological characteristics of MWCNT and CuO used in this study. The volume concentration of the nanoparticles that need to disperse into the base fluid is calculated using the equation (1) given by Ali Akbar and Farhad (1) it has been calculated and presented in the below Table 2.

$$\phi = \frac{\left(\frac{m}{\rho}\right) MWCNT \, + \, \left(\frac{m}{\rho}\right) CuO}{\left(\frac{m}{\rho}\right) MWCNT \, + \, \left(\frac{m}{\rho}\right) CuO \, + \left(\frac{m}{\rho}\right) DI\ water} \times 100 \qquad \text{Eq. 1}$$

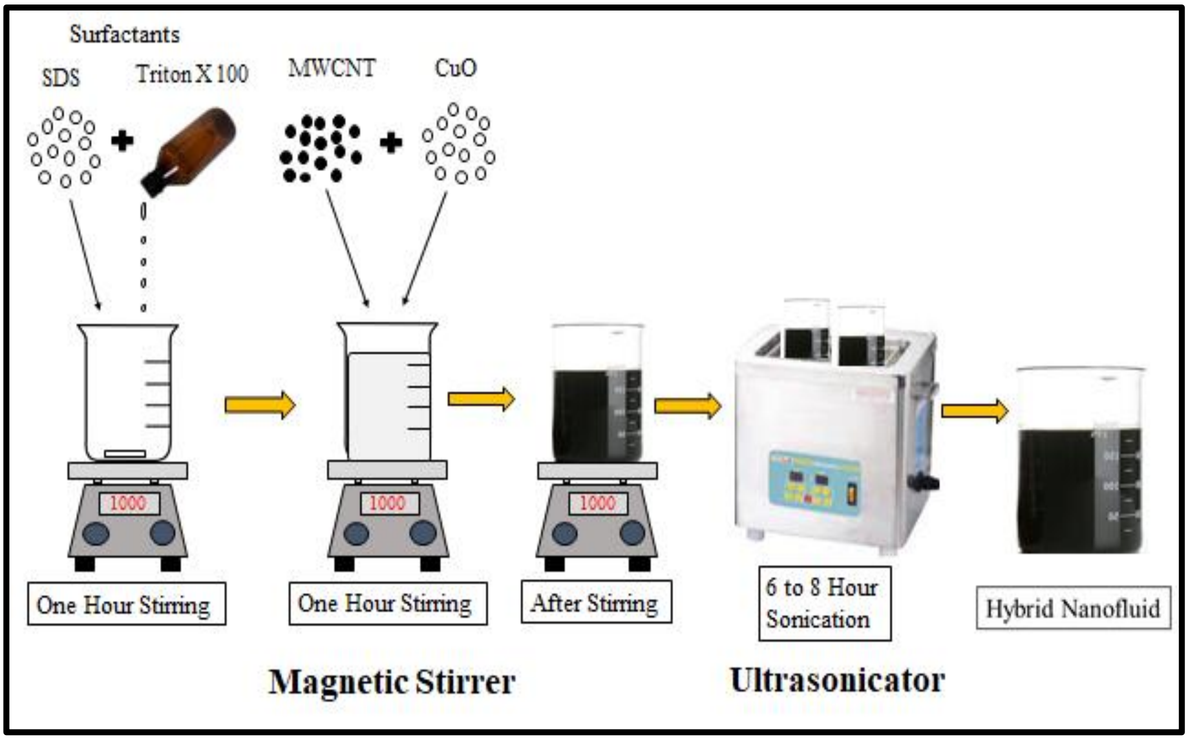

Fig. 1. Preparation of MWCNT/CuO DI water hybrid nanofluid.

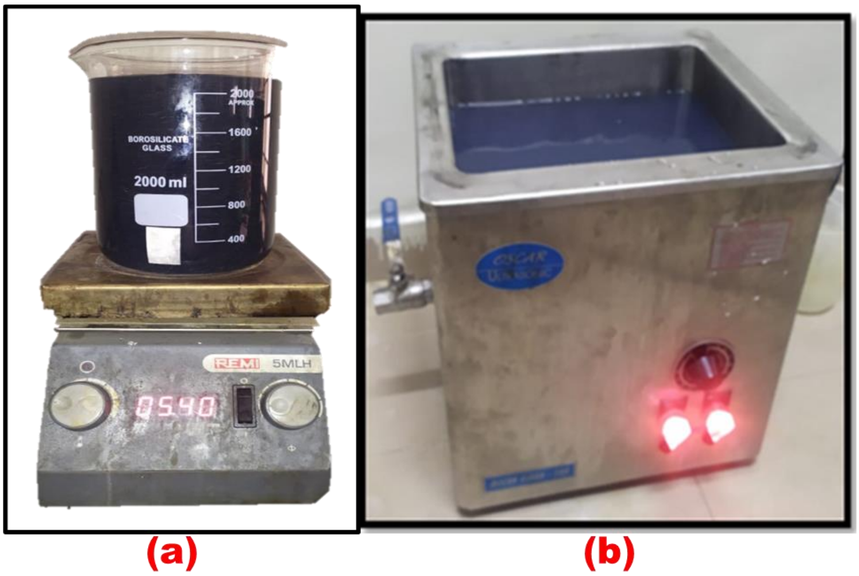

Fig. 2. (a) Magnetic stirrer, (b) Ultrasonic processor.

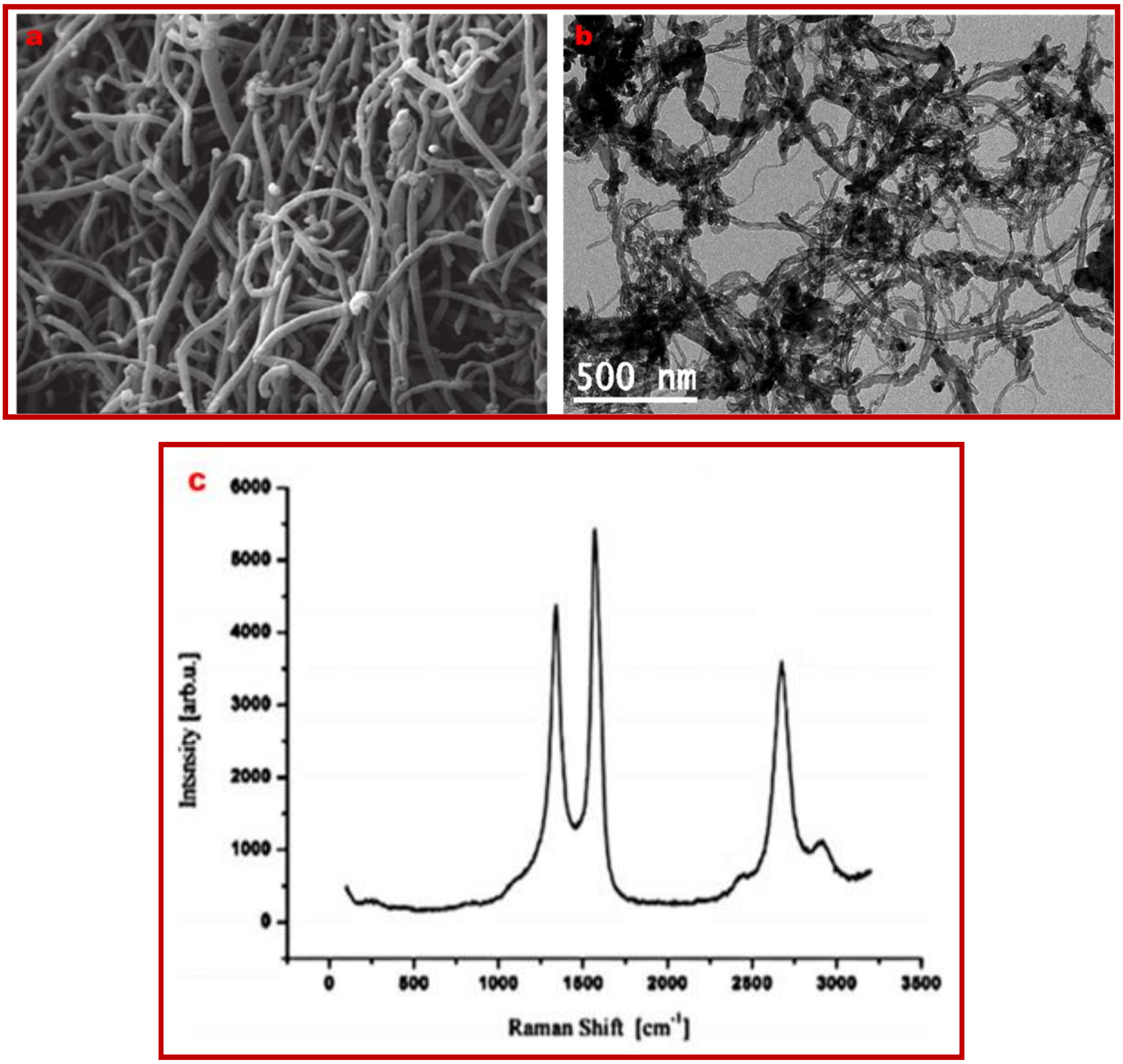

Fig. 3. (a): SEM image of MWCNT nanoparticles (b): TEM image of MWCNT nanoparticles (c) XRD pattern of MWCNT nanoparticles.

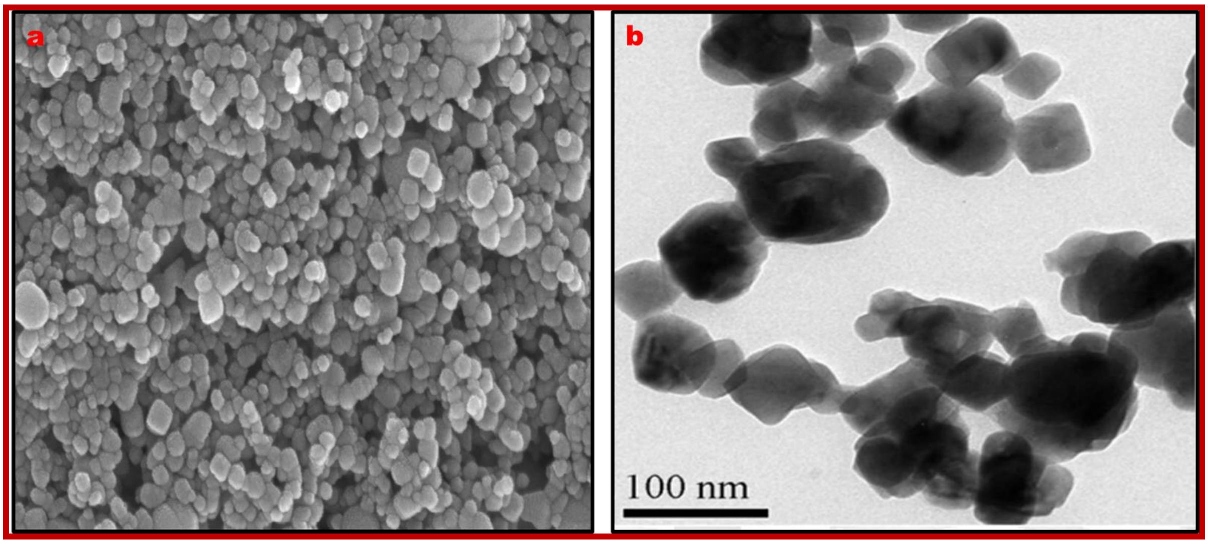

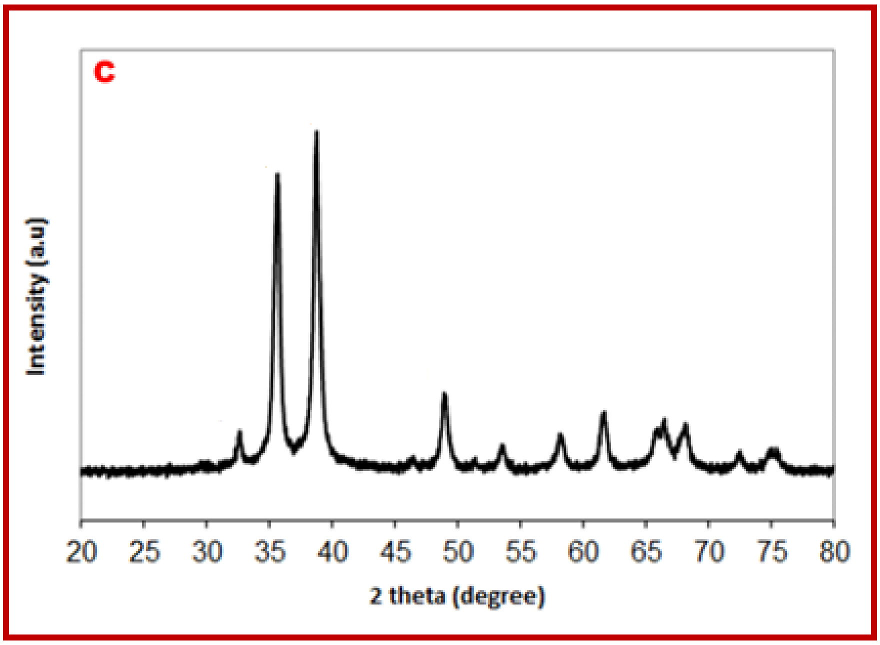

Fig. 4. (a): SEM image of CuO nanoparticles (b): TEM image of CuO nanoparticles
(c) XRD pattern of CuO nanoparticles

Table 1. Properties of MWCNT and CuO.

SPECIFICATION	**MWCNT**	**CuO**
Color	Black	Brownish black
Particle size	10-15 nm	50 nm
Thermal conductivity	3000 W/m. K	76.5 W/m. K
Purity	>97%	99%
Density	2100 kg/m^3	6400 kg/m^3

Table 2. Mass of MWCNT/CuO nanoparticles for different volume fraction.

Quantity of base fluid (DI-water) in Litre	Volume Concentration ϕ in %	Mass of Nanoparticles in grams MWCNT: CuO	MWCNT: CuO and SDS: Triton X-100 ratio
1	0.1	1.582	1:1
1	0.2	3.16	1:1
1	0.3	4.75	1:1
1	0.4	6.35	1.1

2.2 Experimental set up and procedure

The schematic of the experimental setup of concentric heat exchanger with perforated disk inserts for measuring the heat transfer rate and pressure drop characteristics is depicted in the Fig. 5. The test loop consists of a concentric tube heat exchanger, hot water, and cold-water tank, two rotameters with ± 2% accuracy for measuring and to control the flow rate. 9 K type thermocouples with ± 0.1% precision connected to data logger is fixed at different arrangements of heat exchanger to measure both cold water and hot water temperature. Two centrifugal water pumps are used for circulation of both the working fluids and to supply thermal energy to the nano fluid 1.5 kW electric heater is installed to the hot water tank. A manometer connected to the pressure taps at the inlet and outlet of the heat exchanger was used to measure the pressure drop over the test section under isothermal flow conditions. Two central tubes were used to create the heat transfer section. The inner tube was made from copper with 19.05 mm inner diameter, 20.05 mm outer diameter with length of 2000 mm and the annular tube is made up of 50.8 mm inner diameter and 52.8 mm outer diameter of stainless steel with length of 1500 mm as illustrated in Fig 6. According to equation ($Le/D \approx 4.4 \times Re^{1/6}$) [42] the length of the tube to create fully developed turbulent flow at a Reynolds number of 4000-9000. Geometrical specifications of the heat exchanger are exactly listed in Table 3. In this segment of concentric tube heat exchanger, baffles with perforated concentric disks were placed inside the copper and annular stainless-steel tube. Four disk made from copper with an outer diameter 19.05 mm, inner diameter of 9.53 mm and 3 mm of ten small holes on disk are placed inside copper pipe at identical distance as presented in Fig. 7 (a). Similary, for annular tube three outer disk made from copper with identification of outer diameter 50.8 mm, inner diameter 20.05 mm and 9 mm nine holes on disk are placed inside the annulus as demonstrated in Fig. 7 (b).

To reduce radial heat loss to the surroundings, a coating of glass-wool with 10 cm thick and asbestos rope was added to the outside of the heat transfer section and thermocouples. The test section's pressure taps were placed around 50 mm upstream and 150 mm downstream of it, with roughly 1000 mm between them. Within the heat exchanger, the flow channels of two working fluids were placed in counter-flow. In this experiment, the main aim was to know about the heat absorption capability of hybrid nanofluid. In such condition, hot water passes through the annulus while the cold hybrid nanofluid (MWCNT/CuO nanofluids) flows through the tube in the counter-flow direction. Fig. 8 depicts a block diagram of the heat absorption process from hot fluid to cold fluid in a concentric tube heat exchanger with perforated disc inserts. In this study, it was tested for four volume concentrations: 0.1%, 0.2%, 0.3%, and 0.4% at three different flow rates: 200

LPH, 300 LPH, and 400 LPH with cold water temperature was regulated at 25°C; the hot water flow rate is set at 150 LPH. During experimental conduction, the hot water (70 °C) enters at the annulus side (shell side) at a flow rate of 150 LPH, while at the same time, cold hybrid nanofluids enter the counter flow into the tube side (pipe side) at a different flow rate of 200 LPH, 300 LPH, and 400 LPH, respectively. The heat transfer experiment was conducted under a uniform heat flux. At steady state, all data were collected; Hot water flow rate, nanofluid flow rate, temperatures, and manometer column heights were among the critical characteristics is examined. A main valve and a bypass line were used to manage the flow rate through the loops. All thermocouples and sensors have a 0.1℃ precision and were calibrated before being mounted to the test section.

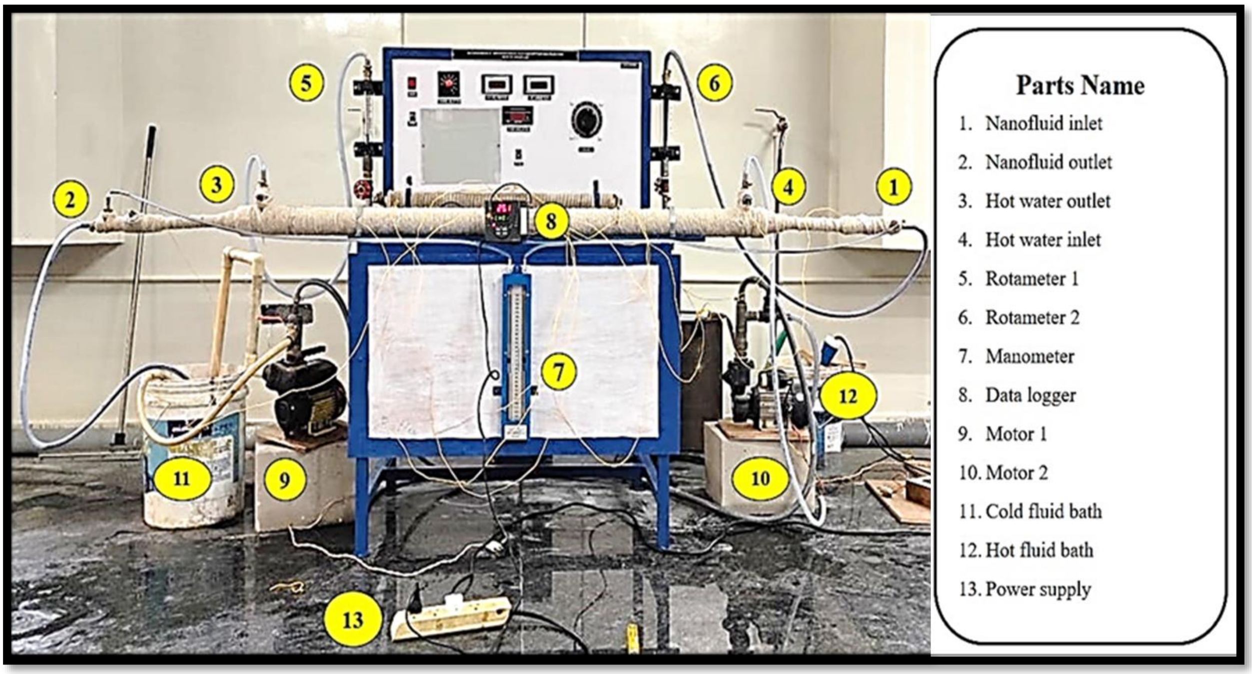

Fig. 5. Experimental setup of concentric heat exchanger with perforated disk inserts.

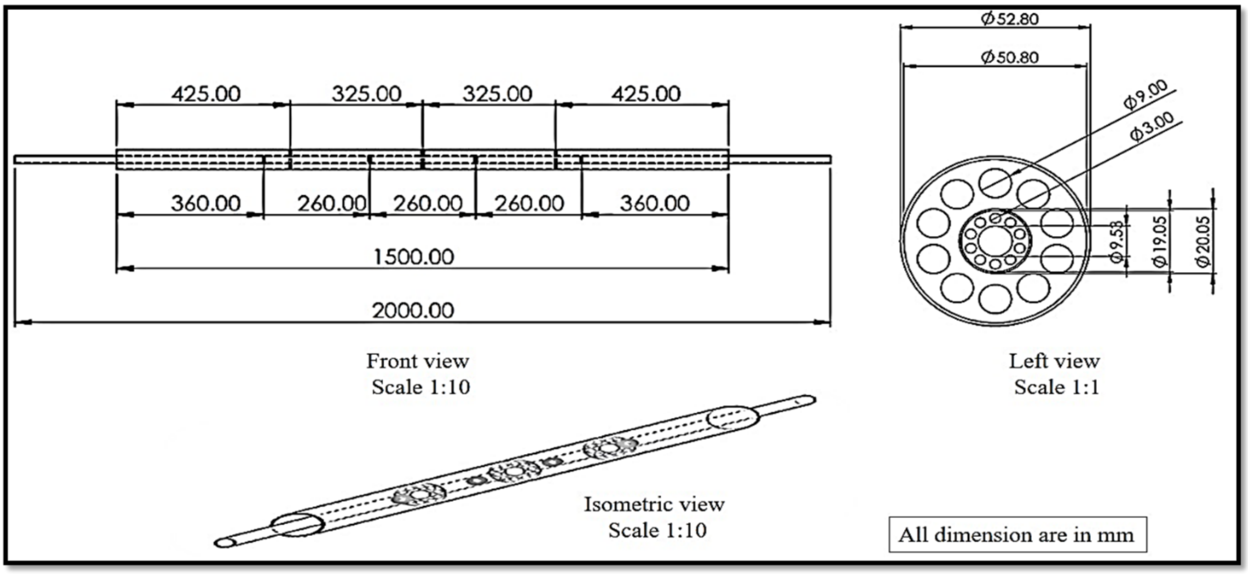

Fig. 6. 2-D and Isometric view of perforated disk inserted DPHE.

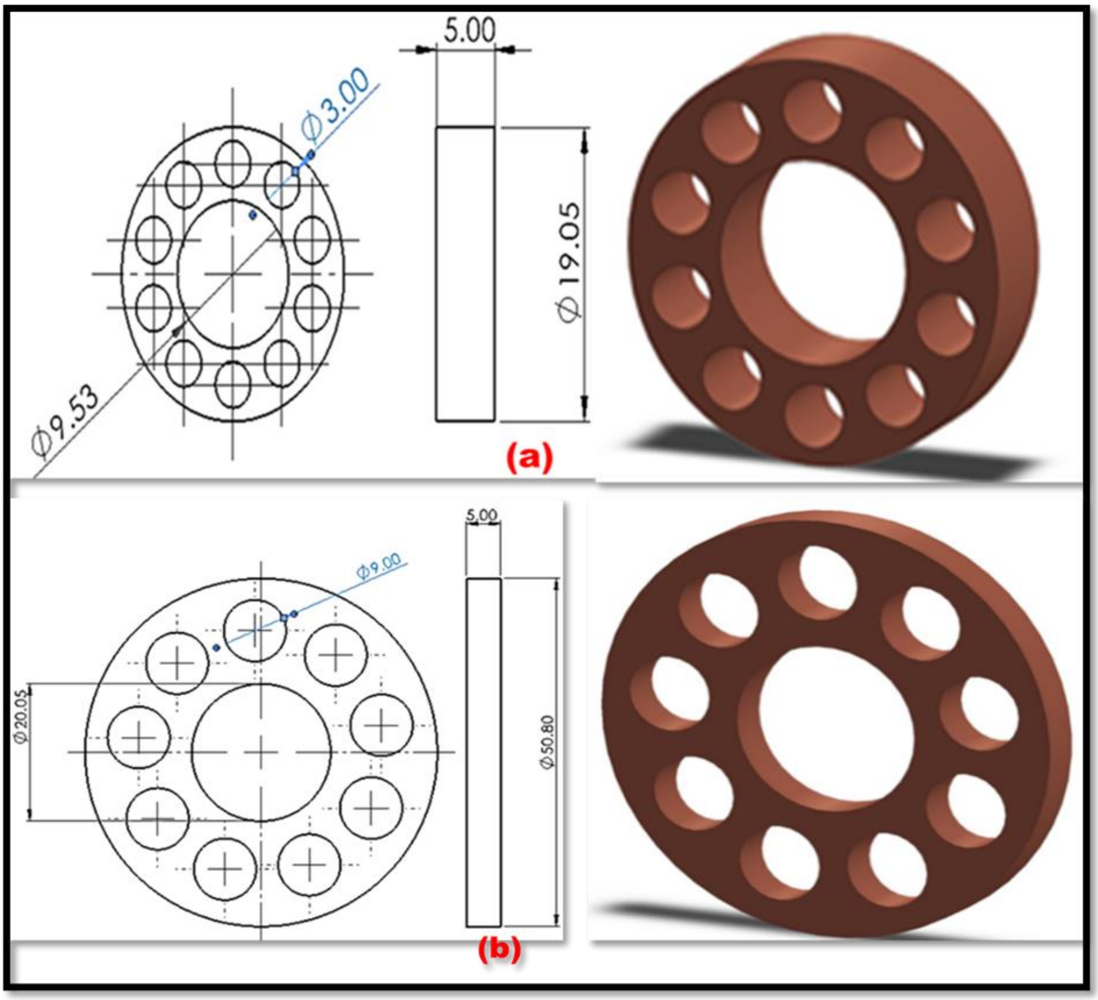

Fig. 7. (a) Dimensions of inner disk inserted in inner tube, (b) Dimensions of outer disk inserted in annuls.

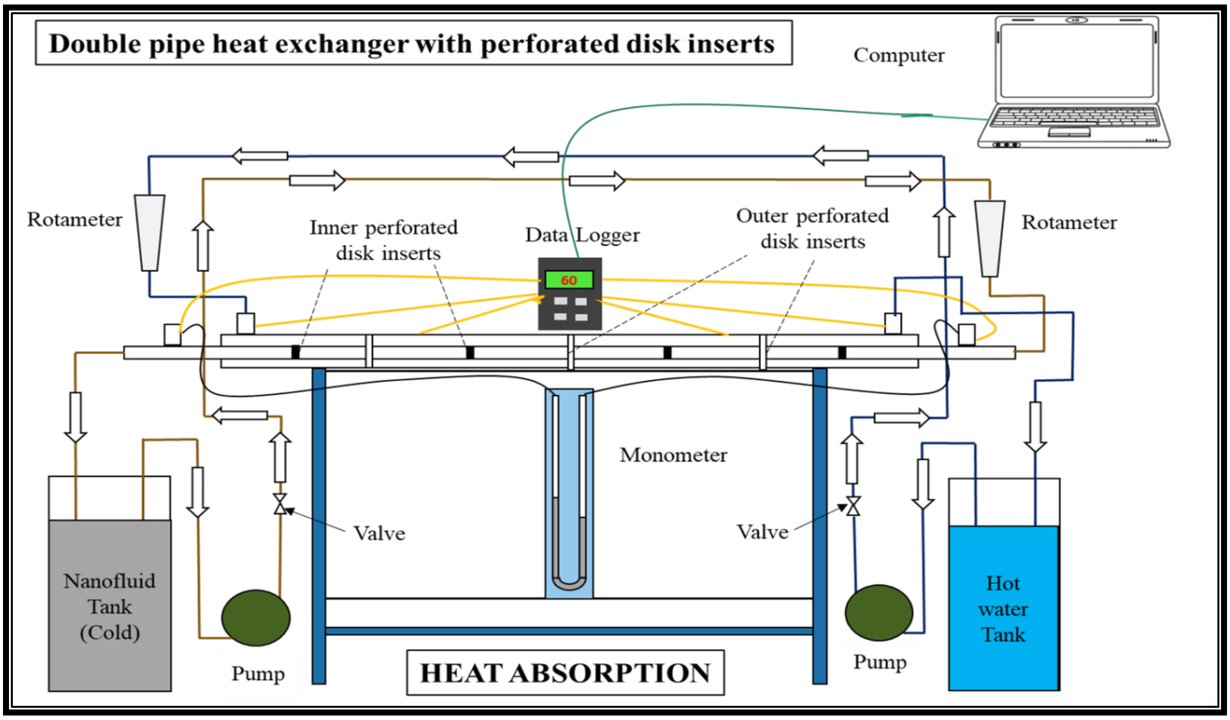

Fig. 8. Block diagram of double pipe heat exchanger with perforated disk inserts.

Table 3. Specification of heat exchanger.

Components	Material	Inner Diameter	Outer Diameter	Length
Outer tube	Stainless steel	50.8 mm	52.8 mm	1500 mm
Inner tube	Copper	19.05 mm	20.05 mm	2000 mm

3. Data analysis

3.1 Density and Specific heat

The effective density of nanofluid is calculated by equation (2) given by Iman and Mohammad(2). Density of MWCNT/CuO DI water-based hybrid nanofluid at different volume concentration.

$$\rho_{nf} = (1 - \emptyset)\rho_{bf} + \emptyset_1\rho_1 + \emptyset_2\rho_2 \qquad \text{Eq. 2}$$

Iman and Mohammad (2) represented an equation (3) to find the specific heat $C_{p,hnf}$ of MWCNT/CuO DI water based hybrid nanofluid at different volume concentration. Thermal equilibrium between the nanoparticles and base fluid assumed by this correlation.

$$C_{p,hynf} = \frac{(1-\emptyset)\rho_{bf}C_{p,bf} + \emptyset_1\rho_1 C_{p1} + \emptyset_2\rho_2 C_{p2}}{\rho_{hynf}} \quad \text{Eq. 3}$$

3.2 Dynamic viscosity

Hayat and Nadeem (3) proposed for viscosity of hybrid nanofluid volume concentration. The dynamic viscosity of MWCNT/CuO DI water-based hybrid nanofluid is calculated by equation (4) Dynamic viscosity of hybrid nanofluid at different volume concentration.

$$\mu_{hynf} = \frac{\mu_{bf}}{(1-\emptyset_1)^{2.5}.\ (1-\emptyset_2)^{2.5}} \quad \text{Eq. 4}$$

3.3 Thermal conductivity

To determine the thermal conductivity of hybrid nanofluid Hayat and Nadeem (3) is used. Thermal conductivity of MWCNT/CuO DI water-based hybrid nanofluid determine by the equation (5).

$$K_{nf} = \frac{K_{CuO} + 2K_f - 2\emptyset_{CuO}(K_f - K_{CuO})}{K_{CuO} + 2K_f + \emptyset_{CuO}(K_f - K_{CuO})} \times K_f \quad \text{Eq. 5}$$

$$K_{hynf} = \frac{K_{MWCNT} + 2K_{nf} - 2\,\emptyset_{MWCNT}(K_{nf} - K_{MWCNT})}{K_{MWCNT} + 2K_{nf} + \emptyset_{MWCNT}(K_{nf} - K_{MWCNT})} \times K_{nf}$$

3.4. Calculation methods

The heat absorption by cold fluid and the heat supplied by the hot fluid are determined by ,

Heat transfer rate of cold fluid (hybrid nanofluids)

$$Q_{nf} = M_{nf}C_{p,nf}(T_{co} - T_{ci})\ in\ W \quad \text{Eq. 6}$$

Heat transfer rate of hot water

$$Q_w = M_w C_{p,w}(T_{hi} - T_{ho})\ in\ W \quad \text{Eq. 7}$$

Average heat transfer rate is calculated.

$$Q_{avg} = \frac{Q_w + Q_{nf}}{2} \quad in\ W$$ Eq. 8

Reynolds number is defined as

$$(R_e)_{nf} = \left(\frac{\rho v D}{\mu}\right)_{nf}$$ Eq. 9

The following equations were used to compute the convective heat transfer coefficient and Nusselt number for nanofluid:

Tube wall temperature with perforated disk inserts

$$T_{wall} = \frac{T_{hi} + T_{i1} + T_{i2} + T_{i3} + T_{ho}}{5} \text{ in °C}$$ Eq. 10

Tube wall temperature without perforated disk inserts.

$$T_{wall} = \frac{T_{hi} + T_{ho}}{2}, \text{ in °C}$$ Eq. 11

Bulk mean temperature

$$T_b = \frac{T_{ci} + T_{co}}{2}, \text{ in °C}$$ Eq. 12

Heat transfer coefficient

$$h = \frac{Q_{avg}}{A_{i\,(T_{wall} - T_b)}} \quad in\ {}^{W}\!/_{m^2 K}$$ Eq. 13

Nusselt number

$$N_u = \frac{h\ D}{K_{nf}}$$ Eq. 14

Theoretical friction factor for nanofluids

$$f_{nf} = 0.961\ \emptyset^{0.052} R_e^{-0.375}$$ Eq. 15

Theoretical friction factor for water

$$f = 0.448 R_e^{-0.275} \quad \text{Eq. 16}$$

Theoretical pressure drop

$$\Delta P = f\left[\frac{L\,\rho\,v^2}{2\,D}\right] \quad \text{Eq. 17}$$

Practical pressure drops.

$$\Delta P = \rho g h \quad \text{Eq. 18}$$

Thermal performance factor

$$R = \left(\frac{N_{unf}}{N_{uf}}\right) \Big/ \left(\frac{f_f}{f_{nf}}\right)^{0.333} \quad \text{Eq. 19}$$

4. Result and discussion

4.1. Stability

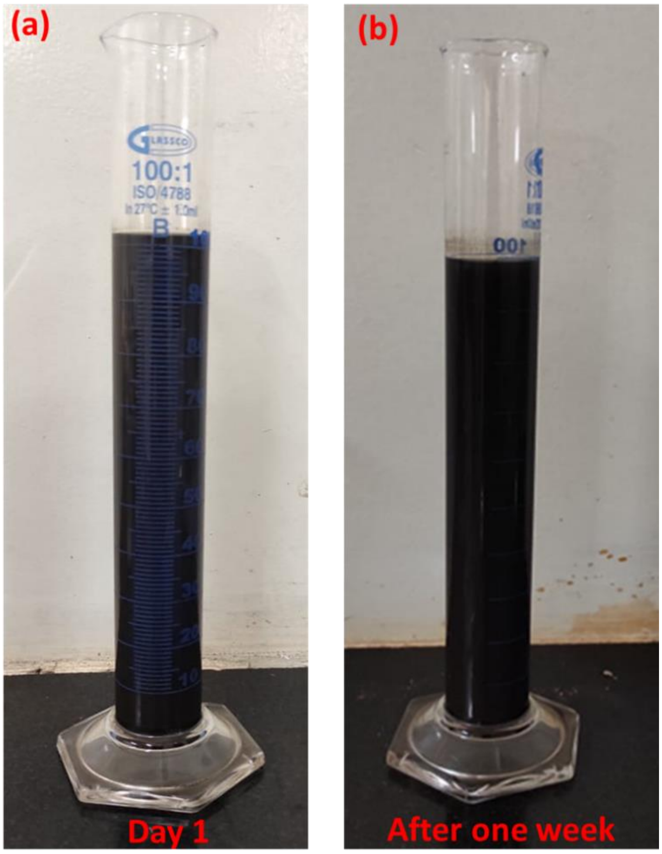

Fig. 9. Images of stability 0.3% volume fraction of hybrid nanofluid at Day one and after one week.

For the preparation of the 0.3% volume fraction of HyNF, MWCNT, and CuO were added at a 1:1 ratio to the DI water as base fluid, and surfactants SDS and Triton X-100 were also added at an equal ratio. Experiment results show that adding surfactants like SDS and Triton X-100 in a 1:1 ratio to the mass of the total nanoparticles gives stability and the finest hybrid particles in water-based fluids. The thermophysical properties of the base fluid can be improved by using two different kinds of nanoparticles. Fig. 9 shows that after a week, there has been no particle agglomeration or sedimentation in the base fluid. MWCNT nanofluid was more stable than CuO nanofluid, which was less stable. In addition, CuO nanoparticle deposition velocity rises over time. CuO nanoparticles were absorbed and suspended by MWCNT when these two nanofluids were combined. As seen in Fig. 9, the samples appear to be homogenous, which should be emphasized.

4.2. Density of MWCNT/CuO DI water hybrid nanofluid at different volume concentration.

The density of the synthesised MWCNT/CuO DI water samples of hybrid nanofluids at different volume concentrations is displayed in Fig. 10. The density of the samples increases as the volume concentration increases. This is due to an increase in the concentration of nanoparticles suspended in the base fluid. Another study found a similar finding, in which the density of the samples increases for the produced Al_2O_3-CuO hybrid nanofluid samples with enhanced volume concentrations of nanoparticles [40].

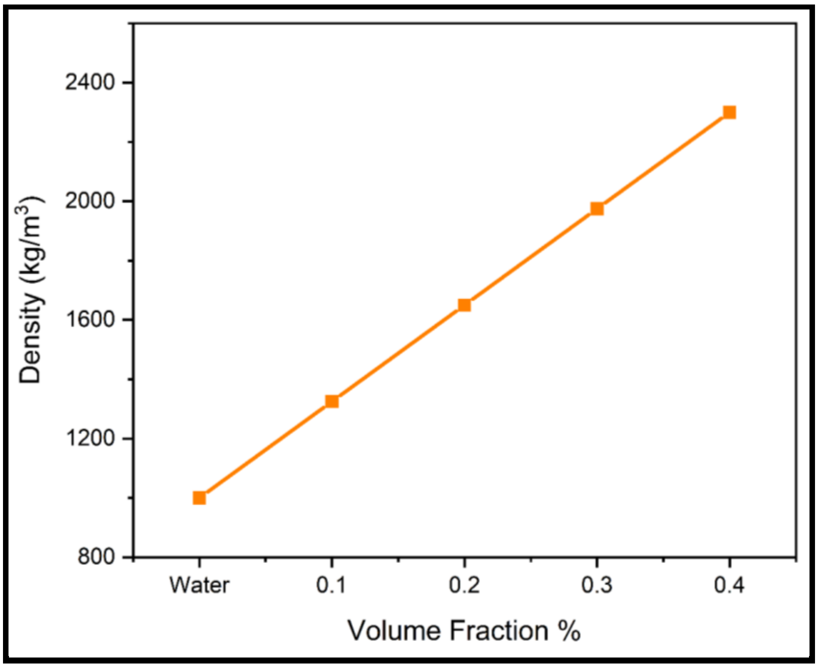

Fig. 10. Density of MWCNT/CuO DI water hybrid nanofluid samples against varying volume concentrations.

4.3. Specific heat of MWCNT/CuO DI water hybrid nanofluid at different volume concentration.

Fig. 11 depicts the specific heat capacity of MWCNT/CuO DI water samples of hybrid nanofluids at different volume concentrations. The specific heat capacity of the samples diminishes as the volume concentration increases. This indicates that the rate of heat absorption and loss in the nanofluid will increase as the concentration of nanoparticles in the base fluid increases. Because when thermal diffusivity increases as a result of nanofluids, their specific heat capacity decreases and it reduces lower than that of water. The results of the current study in relation to nanoparticle volume concentration and specific heat capacity are similar to those of previous studies [44–46].

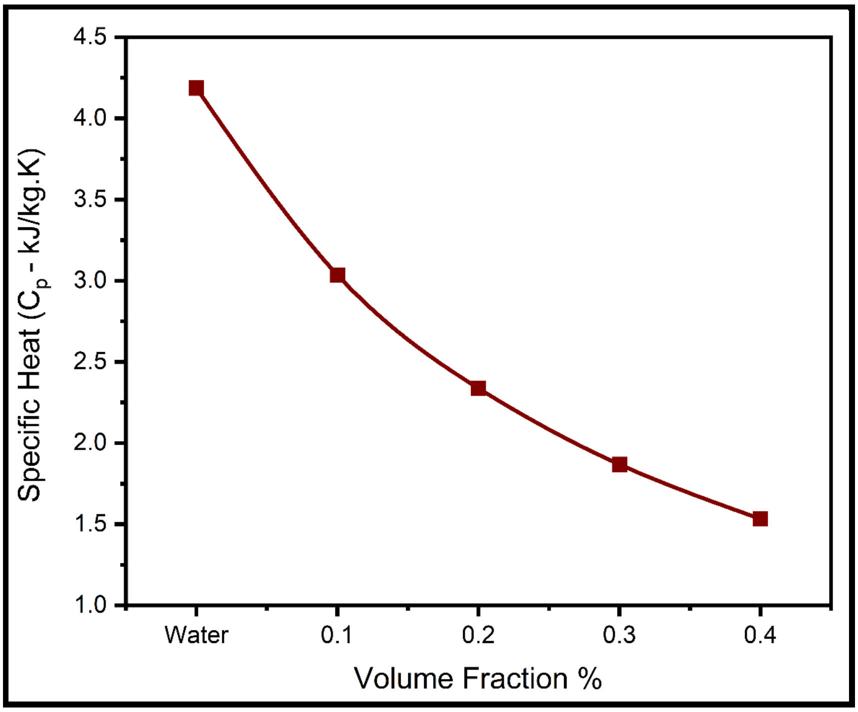

Fig. 11. Specific heat capacity of MWCNT/CuO DI water samples of hybrid nanofluids at different volume concentrations.

4.4. Thermal conductivity of MWCNT/CuO DI water hybrid nanofluid at varying volume concentration

Fig. 12 describes the thermal conductivity of hybrid nanofluid samples as a function of concentration. The the nanofluid samples of thermal conductivity rises as volume concentrations increase. As the number of nanoparticles suspended in the base fluid rises, so does the working fluid's overall surface area. An rise in Brownian movements within hybrid nanofluid samples is another reason for this trend. The random movement of particles floating in a fluid is known as Brownian movement. An earlier investigation concentrated on how Brownian motion affected the thermal conductivity measurements of nanofluids. The higher thermal conductivity of nanofluids is discovered to be indirectly caused by an increase in Brownian movement. By neglecting the Brownian motion particle effect in these models, it is possible to explain the disparities between theoretical and practical results [40].

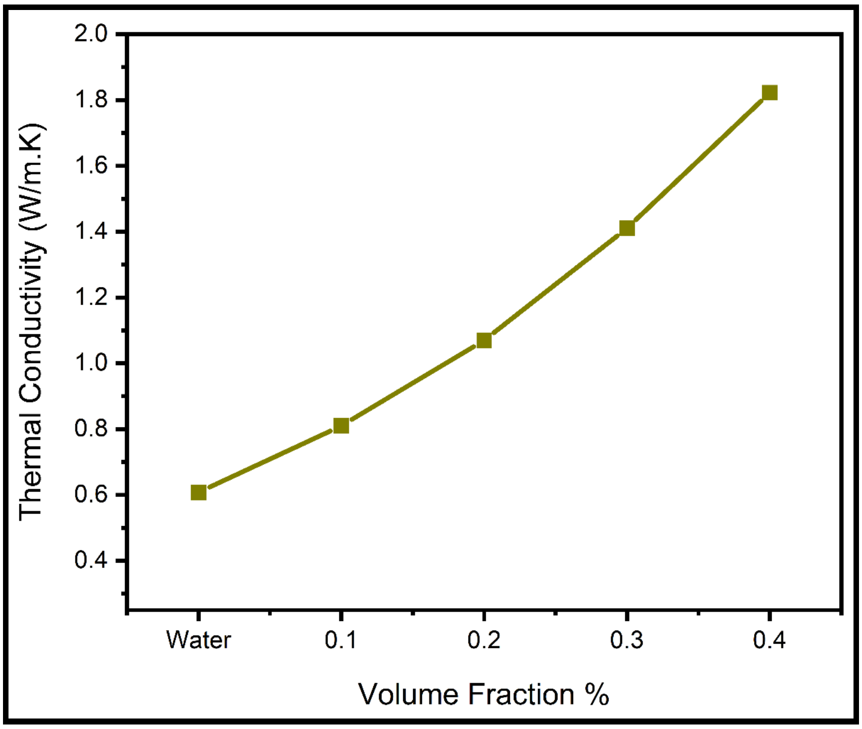

Fig. 12. Thermal conductivity of MWCNT/CuO DI water hybrid nanofluid samples against varying volume concentrations.

4.5. Dynamic viscosity of MWCNT/CuO DI water hybrid nanofluid at different volume concentration.

The findings of an experimental study examining the volume concentration vs viscosity of MWCNT/CuO DI water nanofluid samples are displayed in Fig. 13. The two main factors that determine a nanofluid's viscosity are the viscosity of the base fluid and the volume concentration of nanoparticles. The viscosity of the nanofluid increases along with the concentration of nanoparticles. To employ nanofluid for heat transfer, high viscosity values increase pressure drops and subsequently pumping power, which is not acceptable. In general, excellent stability, good surfactant composition, and good preparation cannot significantly improve viscosity. Similar findings from earlier studies examining the hybrid nanofluid's viscosity at various volume concentrations were found [30, 40, 47].

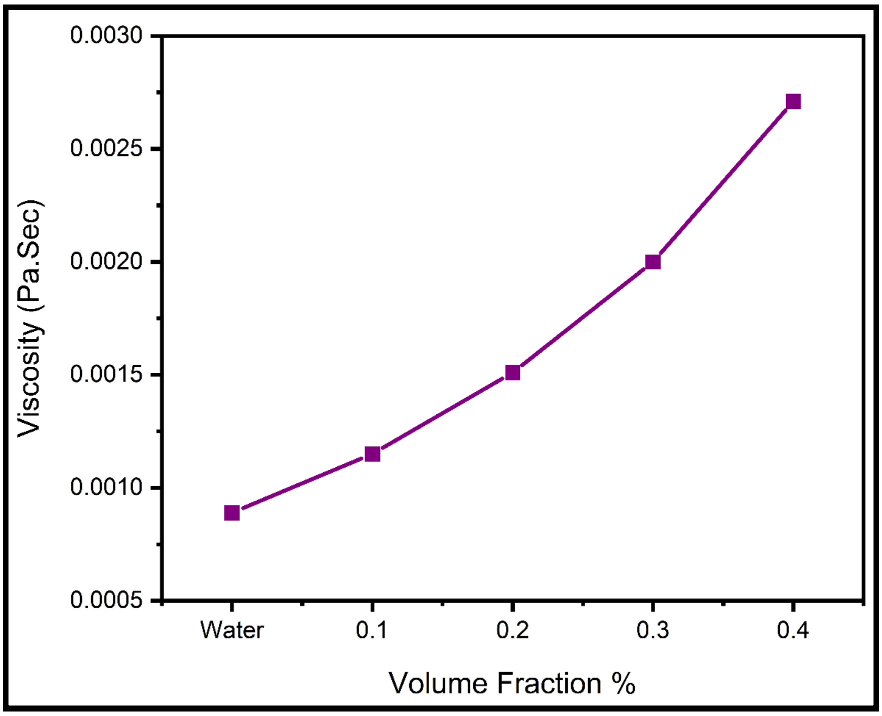

Fig. 13**.** Specific heat capacity of MWCNT/CuO DI water hybrid nanofluid samples against varying volume concentrations.

4.6. Heat transfer coefficient with mass flow rate variations

The typical heat transfer coefficient (HTC) of the nanofluids at different flowrate at varying volume concentrations is presented in Fig. 14. The heat transfer coefficient enhances as the flowrate increases. The HTC values of the MWCNT/CuO hybrid nanofluid samples are greater across all volume concentrations when compared to the base fluid mixture. When compared to 0.2%, 0.1%, 0.4%, volume concentration, and DI water, the biggest augmentation in terms of HTC values is 11.08%, 16.16%, 27.16%, and 46.11% when employing hybrid nanofluid samples at 0.3% volume concentration. The hybrid nanofluid samples show a highest increase of 18.14% HTC when compared to the base fluid mixture. To justify the use of nanofluids in practical applications, it is critical to assess their friction properties in addition to measuring their heat transfer characteristics. The incorporation of MWCNT/CuO nanoparticles into a base mixture of DI water (50:50) has been found to improve the fluid's overall heat transfer capability. Similar results have been discovered in other study efforts, which support the current work's findings and observations [48-50].

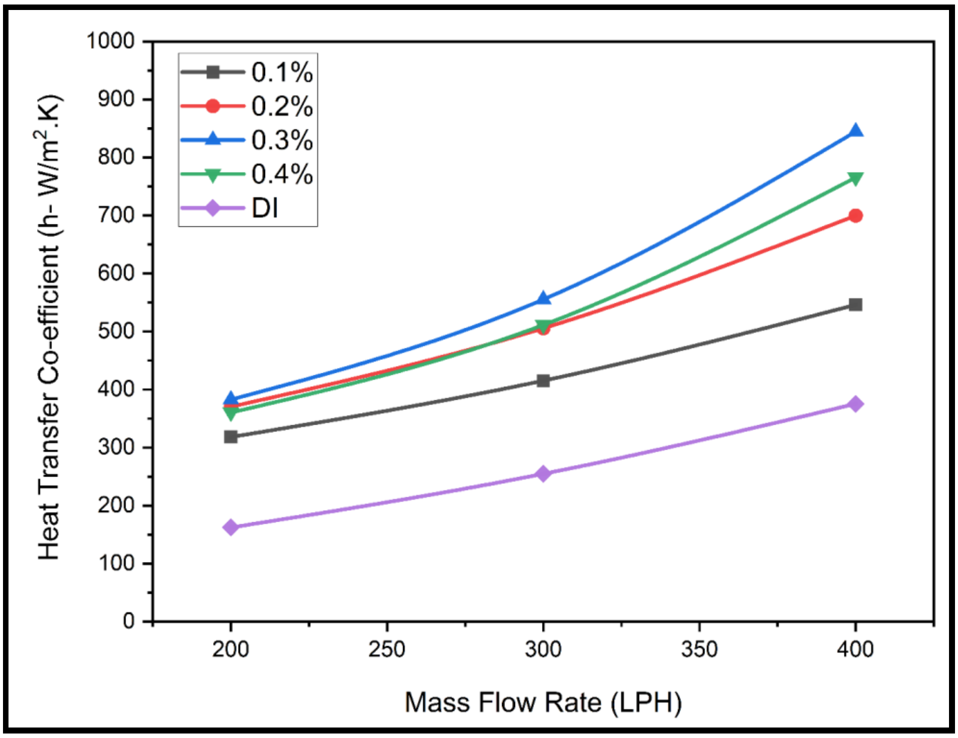

Fig. 14. For both DI water and hybrid Nanofluid samples, the average heat transfer coefficient vs flowrate was calculated for different Volume concentration.

4.7. Nusselt number with mass flow rate variations

The average Nusselt number and flowrate for various hybrid nanoparticle volume fractions of 0.1%, 0.2%, 0.3%, and 0.4% in comparison to the base fluid are displayed in Fig. 15. The Nusselt number at the fluid boundary layer shows the proportion of convection to conduction heat transfer. A higher Nusselt number denotes an increase in active convectional heat transport. The results show that the cold working fluid's Nusselt number rises as the Reynolds number rises, and that at a given Reynolds number, the Nusselt number rises as the volume concentration of nanoparticles increases. It is evident that the maximum enhancement of the nanofluid Nusselt number at 0.3 vol% occurred at the highest tested Reynolds number. The maximum enhancement of the nanofluid Nusselt number at 0.1%, 0.2%, 0.3%, and 0.4% particle volume concentrations are specified at approximately 13.7, 18.9, 28.54, and 9.8%, respectively. These improvements could be the result of a number of factors, such as the addition of MWCNT/CuO Hybrid nanoparticles increasing the base fluid's thermal conductivity, a decrease in the thickness of the boundary layer, Brownian motion of the nanoparticles, and the creation of friction force between the fluid and the particles. The high thermal conductivity values of the hybrid nanofluids, which are the source of this trend, are in line with the findings of earlier researchers [51,52].

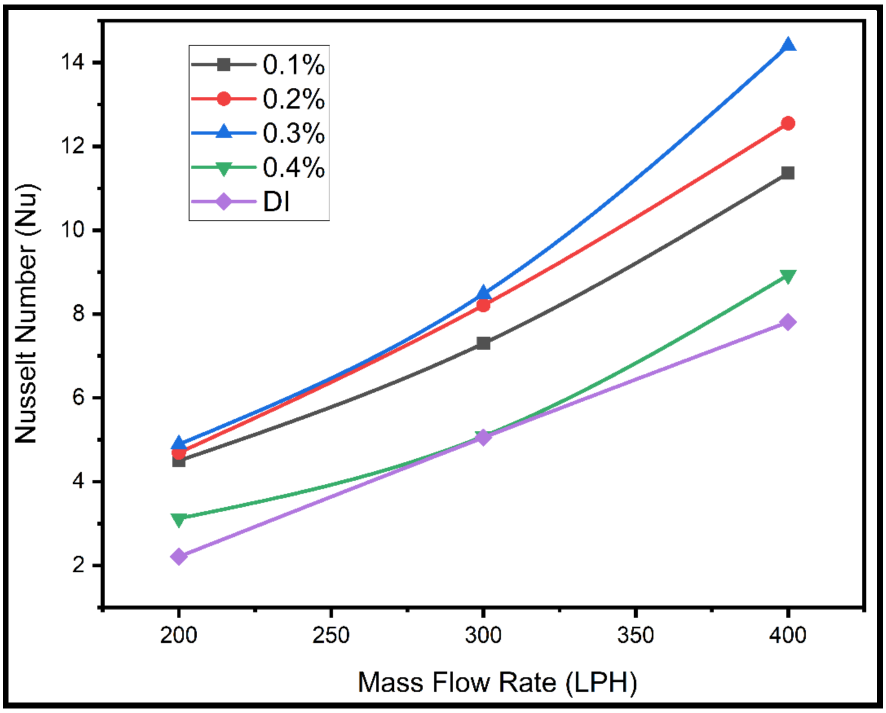

Fig. 15**.** For both DI water and hybrid Nanofluid samples, the average Nusselt number vs flowrate was calculated for different volume concentration.

4.8. Pressure drops with mass flow rate variations.

Nanofluids must be developed to improve heat transmission while minimising pressure drop to be successful in practical applications. As a result, the pressure drops of the MWCNT/CuO Hybrid DI water nanofluid in a tube with perforated disc inserts are experimentally evaluated under isothermal circumstances for turbulent flow. According to Fig. 16, an increase in Reynolds number and nanoparticle concentration at a constant surfactant concentration hybrid nanofluid results in a modest rise in pressure drop in perforated disc inserts HE. This is due to an increase in nanofluid viscosity caused by a rise in NP volume concentrations, which speeds up the agglomeration process and settling of nanoparticles in the heat exchanger, resulting in a larger pressure drop. At the current experimental conditions, there is a considerable increase in pressure drop for the nanofluid when compared to water, indicating that dilute nanofluids will cause an additional cost in pump power. As foams are primarily defined by the characteristics of a thin boundary zone in which surfactants produce slip and the destructive phenomenon of foaming. Also, as the temperature rises, more air can enter the bubbles, speeding up their development and enhancing the pressure drop ratio. It has previously been noted in the literature that the pressure drop was inversely correlated with the volume concentration of nanofluids and volume flow rate [53,54].

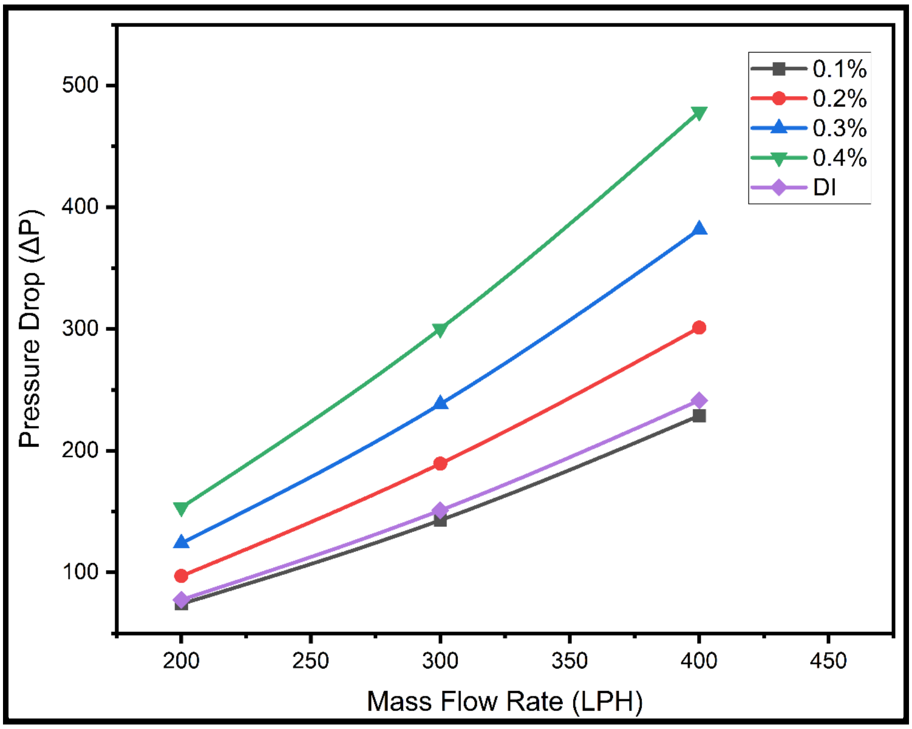

Fig. 16. For both DI water and hybrid Nanofluid samples, the Pressure drop vs flowrate was calculated for different volume concentration.

4.9. Friction factor with mass flow rate variations

Fig. 17 illustrate the friction factor results for different mass flowrate for all the prepared fluid samples. In all circumstances, friction factors decrease significantly as flowrate increases. According to Fig. 17, as the volume % of nanoparticles and flowrate of nanofluid both rises, so does the friction factor. When compared to the application of base fluid, the usage of nanofluids generates small increases in friction factor. This demonstrates the attractive feature of using nanofluid for heat transfer augmentation at a negligible cost. When compared to pure water, using nanofluid in a concentric tube heat exchanger with perforated disc inserts results in a 12.56% greater friction factor. This improvement could result from increasing the working fluid mass density and viscosity by introducing and suspending MWCNT/CuO Hybrid nanoparticles in DI water. This could be due to an increase in shear force on the tube wall generated by the increased amount of nanoparticles. Nanofluids with concentrations of 0.1%, 0.2%, 0.3%, and 0.4% by volume concentration appear to have average friction factors that are higher than the base fluid by around 5.66, 7.85, 10.84, and 15.84%, respectively. This trend is consistent with other researchers' findings and is caused by the greater friction factor values of the hybrid nanofluids compared to DI water [55,56].

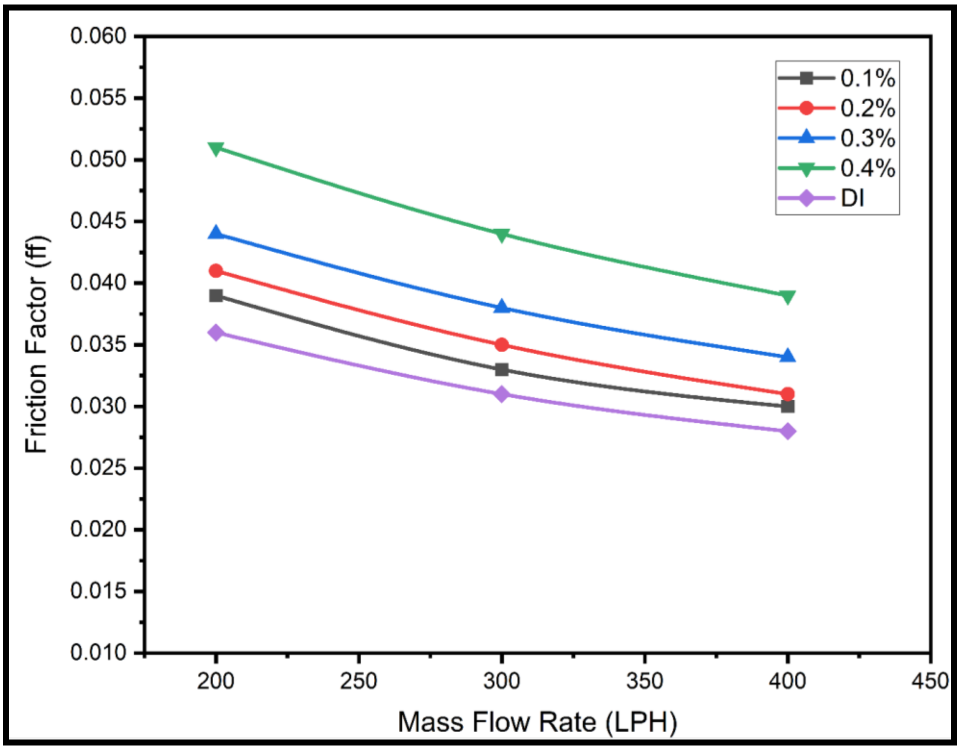

Fig. 17**.** For both DI water and hybrid Nanofluid samples, the Friction factor vs flowrate was calculated for different volume concentration.

4.10. Thermal performance factor with mass flow rate variations

The Nusselt number ratio to the friction factor ratio at the same pumping power is used to establish the thermal performance factor (R) [16]. Fig. 8 shows how the thermal performance factor (R) changes with flowrate for various volume concentrations of MWCNT/CuO hybrid nanoparticles in DI water nanofluid in a perforated disk-inserted concentric heat exchanger. As can be seen, thermal performance improves as flowrate rises. This suggests that using nanofluid and perforated disc inserts to save energy at higher Reynolds numbers in a turbulent regime is possible. Also, the stability of the suspension and the rate of heat transmission are improved by employing the ideal amounts of surfactants in the hybrid nanofluid used. The results also show that as the concentration of nanofluid increases, so does the thermal performance factor. For volume concentrations of 0.1%, 0.2%, 0.3%, and 0.4% for MWCNT/CuO hybrid nanoparticles in DI water nanofluid, the mean improvements in the thermal performance of the perforated disk-inserted concentric heat exchanger are approximately 13.05, 18.37, 28.57, and 7.69%, respectively. This is due to the nanofluid's greater efficiency of heat transfer and disturbance compared to the base fluid at the same pumping power. A nanofluid with a 0.3% concentration performs better thermal performances than others. The use of nanofluid at a

Reynolds number of 8,000 results in a maximum thermal performance factor of 1.68 for the range under consideration [54,57].

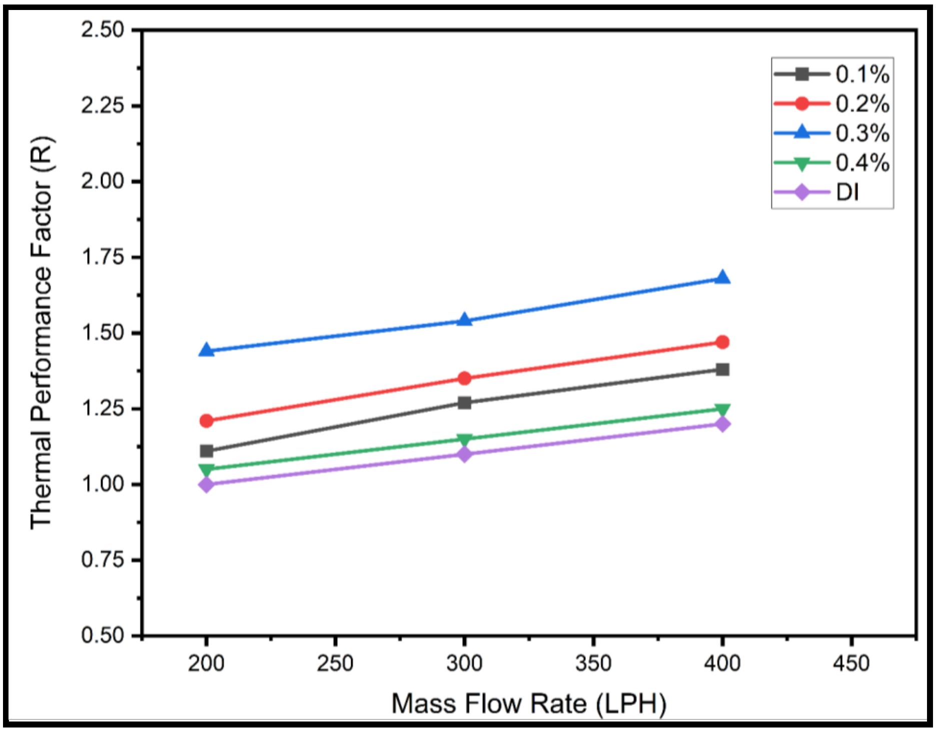

Fig. 18. Comparison of the thermal performance factor of nanofluid at various flowrates and nanoparticle volume percentages in the perforated disc insert heat exchanger.

5. Conclusion

The stability of hybrid nanofluid (HyNF), the behaviour of heat transfer, and the flow of HyNF as a heat absorption fluid in a concentric tube perforated disc inserted heat exchanger were all examined in the current experimental work. Several flow rates and volume concentrations were used for these studies. The following findings were established after an investigation of the impacts of the volume flow rate of cold fluid, the temperature of hot fluid, and the kind of cold fluid on the performance of heat transfer and flowrate:

1. When the differences between the experimental values and the correlation values are within a certain range, the goal of measuring and comparing the fluid properties of the hybrid nanofluids, such as density(ρ), thermal conductivity(K), viscosity(μ), and specific heat capacity (C_p), is met.

2. Also, the second goal of this work, to evaluate the thermal performance of hybrid nanofluid in DI water, has also been accomplished. Based on the results of the current study, the thermophysical fluid properties of the MWCNT-CuO hybrid nanofluid samples may have improved. When compared to base water, the hybrid nanofluid samples can increase the working fluid's thermal conductivity by 34.2%.
3. The Nusselt number (Nu) and total HTC of nanofluid increased as the Reynolds number increased. Moreover, an enhancement in the nanoparticle volume concentration increases both the Nusselt number and the overall HTC at a given Reynolds number. When compared to water, the use of hybrid nanofluids as a working fluid improves the Nusselt number and overall heat transfer coefficient in concentric tube perforated disc inserted heat exchangers by 26.7% and 29.2%, respectively.
4. Some conceivable causes for the increase in heat transfer include the addition of MWCNT-CuO hybrid nanoparticles, which increase the base liquid's thermal conductivity, the friction force between the fluid and the nanoparticles, the Brownian motion of the nanoparticles, and a decrease in the thickness of the boundary layer.
5. Pressure drops, friction factor, and pumping power all increased slightly because of the foaming phenomenon, but no distinct trend was noted.
6. Lastly, the heat exchanger with nanofluid was tested for its thermal performance, and a higher thermal performance factor (R) of about 28.57% at 0.3 vol% was reported.

References

[1] Eastman JA, Choi SU, Li S, Yu W, Thompson LJ. Anomalously increased effective thermal conductivities of ethylene glycol-based nanofluids containing copper nanoparticles. Applied physics letters. 2001 Feb 5;78(6):718-20.

[2] S.U. Choi, J.A. Eastman, Enhancing Thermal Conductivity of Fluids with Nanoparticles, in, Argonne National Lab, IL (United States), 1995.

[3] M.U. Sajid, H.M. Ali, Thermal conductivity of hybrid nanofluids: a critical review, Int. J. Heat Mass Transf. 126 (2018) 211–234.

[4] M.H. Esfe, H. Rostamian, M. Rejvani, M.R.S. Emami, Rheological behavior characteristics of ZrO_2-MWCNT/10w40 hybrid nano-lubricant affected by temperature, concentration, and shear rate: an experimental study and a neural network simulating, Phys. E: Low-dimen. Syst. Nanostruct. 102 (2018) 160–170.

[5] M.H. Esfe, M.R.S. Emami, M.K. Amiri, Experimental investigation of effective parameters on MWCNT–TiO_2/SAE50 hybrid nanofluid viscosity, J. Therm. Anal. Calorim. 137 (2019) 743–757.

[6] M.H. Esfe, H.R. Raki, M.R.S. Emami, M. Afrand, Viscosity and rheological properties of antifreeze based nanofluid containing hybrid nano-powders of MWCNTs and TiO_2 under different temperature conditions, Powder Technol. 342 (2019) 808–816.
[7] M.H. Hamzah, N.A.C. Sidik, T.L. Ken, R. Mamat, G. Najafi, Factors affecting the performance of hybrid nanofluids: a comprehensive review, Int. J. Heat Mass Transf. 115 (2017) 630–646.
[8] L. Yang, W. Ji, M. Mao, J.-n. Huang, An updated review on the properties, fabrication and application of hybrid-nanofluids along with their environmental effects, J. Clean. Prod. 120408 (2020).
[9] N.A.C. Sidik, M.M. Jamil, W.M.A.A. Japar, I.M. Adamu, A review on preparation methods, stability and applications of hybrid nanofluids, Renew. Sust. Energ. Rev. 80 (2017) 1112–1122.
[10] F. Siddiqui, C. Tso, K. Chan, S. Fu, C.Y. Chao, On trade-off for dispersion stability and thermal transport of Cu-Al2O3 hybrid nanofluid for various mixing ratios, Int. J. Heat Mass Transf. 132 (2019) 1200–1216.
[11] Y. Zhai, L. Li, J. Wang, Z. Li, Evaluation of surfactant on stability and thermal performance of Al_2O_3-ethylene glycol (EG) nanofluids, Powder Technol. 343 (2019) 215–224.
[12] I. Mahbubul, R. Saidur, M. Amalina, E. Elcioglu, T. Okutucu-Ozyurt, Effective ultrasonication process for better colloidal dispersion of nanofluid, Ultrason. Sonochem. 26 (2015) 361–369.
[13] S. Sharma, S.M. Gupta, Preparation, and evaluation of stable nanofluids for heat transfer application: a review, Exp. Thermal Fluid Sci. 79 (2016) 202–212.
[14] R.T. Wang, J.-C. Wang, Intelligent dimensional and thermal performance analysis of Al_2O_3 nanofluid, Energy Convers. Manag. 138 (2017) 686–697.
[15] H. Ghorabaee, M.R.S. Emami, M. Shafahi, Effect of Nanofluid and surfactant on thermosyphon heat pipe performance, Heat Transf. Eng. (2019) 1–14.
[16] I. Fazeli, M.R. Sarmasti Emami, M.H. Nazeri, Comparing the effect of single and mixture surfactants on the improvement in stability and thermal conductivity of CuO nanofluid: an experimental study. J. Therm. Anal. Calorim. (2020), https://doi.org/10.1007/s10973-020-10056-8.
[17] X. Li, D. Zhu, X. Wang, N. Wang, J. Gao, H. Li, Thermal conductivity enhancement dependent pH and chemical surfactant for Cu-H_2O nanofluids, Thermochim. Acta 469 (2008) 98–103.
[18] V. Kumar, A.K. Tiwari, S.K. Ghosh, Application of nanofluids in plate heat exchanger: a review, Energy Convers. Manag. 105 (2015) 1017–1036.
[19] N.S. Pandya, H. Shah, M. Molana, A.K. Tiwari, Heat transfer enhancement with nanofluids in plate heat exchangers: a comprehensive review, Eur. J. Mech.-B/Fluids 81 (2020) 173–190.
[20] A.K. Tiwari, P. Ghosh, J. Sarkar, Performance comparison of the plate heat exchanger using different nanofluids, Exp. Thermal Fluid Sci. 49 (2013) 141–151.
[21] D. Huang, Z. Wu, B. Sunden, Pressure drop and convective heat transfer of Al_2O_3/

water and MWCNT/water nanofluids in a chevron plate heat exchanger, Int. J. Heat Mass Transf. 89 (2015) 620–626.

[22] R. Barzegarian, M.K. Moraveji, A. Aloueyan, Experimental investigation on heat transfer characteristics and pressure drop of BPHE (brazed plate heat exchanger) using TiO_2–water nanofluid, Exp. Thermal Fluid Sci. 74 (2016) 11–18.

[23] B. Sun, C. Peng, R. Zuo, D. Yang, H. Li, Investigation on the flow and convective heat transfer characteristics of nanofluids in the plate heat exchanger, Exp. Thermal Fluid Sci. 76 (2016) 75–86.

[24] A. Behrangzade, M.M. Heyhat, The effect of using nano-silver dispersed water based nanofluid as a passive method for energy efficiency enhancement in a plate heat exchanger, Appl. Therm. Eng. 102 (2016) 311–317.

[25] M. Sarafraz, F. Hormozi, Heat transfer, pressure drop and fouling studies of multiwalled carbon nanotube nano-fluids inside a plate heat exchanger, Exp. Thermal Fluid Sci. 72 (2016) 1–11.

[26] T.-P. Teng, T.-C. Hsiao, C.-C. Chung, Characteristics of carbon-based nanofluids and their application in a brazed plate heat exchanger under laminar flow, Appl. Therm. Eng. 146 (2019) 160–168.

[27] Z. Wang, Z. Wu, F. Han, L. Wads¨o, B. Sund´en, Experimental comparative evaluation of a graphene nanofluid coolant in miniature plate heat exchanger, Int. J. Therm. Sci. 130 (2018) 148–156.

[28] S. Pourhoseini, N. Naghizadeh, H. Hoseinzadeh, Effect of silver-water nanofluid on heat transfer performance of a plate heat exchanger: an experimental and theoretical study, Powder Technol. 332 (2018) 279–286.

[29] Z. Li, M.M. Sarafraz, A. Mazinani, T. Hayat, H. Alsulami, M. Goodarzi, Pool boiling heat transfer to CuO-H2O nanofluid on finned surfaces, Int. J. Heat Mass Transf. 156 (2020), 119780.

[30] D. Huang, Z. Wu, B. Sunden, Effects of hybrid nanofluid mixture in plate heat exchangers, Exp. Thermal Fluid Sci. 72 (2016) 190–196.

[31] V. Kumar, A.K. Tiwari, S.K. Ghosh, Effect of variable spacing on performance of plate heat exchanger using nanofluids, Energy 114 (2016) 1107–1119.

[32] M. Goodarzi, A. Amiri, M.S. Goodarzi, M.R. Safaei, A. Karimipour, E.M. Languri, M. Dahari, Investigation of heat transfer and pressure drop of a counter flow corrugated plate heat exchanger using MWCNT based nanofluids, Intern. commun. Heat Mass Transf. 66 (2015) 172–179.

[33] A. Bhattad, J. Sarkar, P. Ghosh, Discrete phase numerical model and experimental study of hybrid nanofluid heat transfer and pressure drop in plate heat exchanger, Intern. Commun. Heat Mass Transf. 91 (2018) 262–273.

[34] A. Bhattad, J. Sarkar, P. Ghosh, Experimentation on effect of particle ratio on hydrothermal performance of plate heat exchanger using hybrid nanofluid, Appl. Therm. Eng. 162 (2019) 114309.

[35] Jehhef KA, Siba MA. Effect of surfactant addition on the nanofluids properties: a review. Acta Mechanica Malaysia. 2019;2(2):1-9.

[36] Arani AA, Pourmoghadam F. Experimental investigation of thermal conductivity behavior of MWCNTS-Al_2O_3/ethylene glycol hybrid Nanofluid: Providing new thermal conductivity correlation. Heat and Mass Transfer. 2019 Aug 1;55:2329-39.

[37] Karimipour A, Malekahmadi O, Karimipour A, Shahgholi M, Li Z. Thermal conductivity enhancement via synthesis produces a new hybrid mixture composed of copper oxide and multi-walled carbon nanotube dispersed in water: experimental characterization and artificial neural network modeling. International Journal of Thermophysics. 2020 Aug;41:1-27.

[38] Zadkhast M, Toghraie D, Karimipour A. Developing a new correlation to estimate the thermal conductivity of MWCNT-CuO/water hybrid nanofluid via an experimental investigation. Journal of Thermal Analysis and Calorimetry. 2017 Aug;129:859-67.

[39] Qu J, Zhang R, Wang Z, Wang Q. Photo-thermal conversion properties of hybrid CuO-MWCNT/H2O nanofluids for direct solar thermal energy harvest. Applied Thermal Engineering. 2019 Jan 25;147:390-8.

[40] Fazeli I, Emami MR, Rashidi A. Investigation and optimization of the behavior of heat transfer and flow of MWCNT-CuO hybrid nanofluid in a brazed plate heat exchanger using response surface methodology. International Communications in Heat and Mass Transfer. 2021 Mar 1;122:105175.

[41] Akhgar A, Toghraie D, Sina N, Afrand M. Developing dissimilar artificial neural networks (ANNs) to prediction the thermal conductivity of MWCNT-TiO2/Water-ethylene glycol hybrid nanofluid. Powder Technology. 2019 Oct 1;355:602-10.

[42] F.M. White, Viscous Fluid Flow, McGraw Hill, New York, 2006.

[43] Hayat T, Nadeem S. Heat transfer enhancement with Ag–CuO/water hybrid nanofluid. Results in physics. 2017 Jan 1;7:2317-24.

[44] Na. P.K., K. D.P., D. A., and D. D.K., “Experimental investigation of viscosity and specific heat of silicon dioxide nanofluid,” Micro Nano Lett., vol. 2, no. 3, pp. 67–71, 2007, doi: 10.1049/mnl.

[45] S.A. Angayarkanni, Vijutha Sunny, John Philip, Effect of nanoparticle size, morphology and concentration on specific heat capacity and thermal conductivity of nanofluids, J Nanofluids 4 (3) (2015) 302–309.

[46] R. Hentschke, On the specific heat capacity enhancement in nanofluids, Nanoscale Res. Lett. 11 (1) (2016) 1–11, https://doi.org/10.1186/s11671-015-1188-5.

[47] Mohammadali Baghbanzadeh, Alimorad Rashidi, Amir Hassan Soleimanisalim, Davood Rashtchian, Investigating the rheological properties of nanofluids of water/hybrid nanostructure of spherical silica/MWCNT, Thermochim Acta 578 (2014) 53–58.

[48] M. Nuim Labib, Md. J. Nine, Handry Afrianto, Hanshik Chung, Hyomin Jeong, Numerical investigation on effect of base fluids and hybrid nanofluid in forced convective heat transfer, Int. J. Therm. Sci. 71 (2013) 163–171.

[49] Hyder H. Balla, Shahrir Abdullah, Wan MohdFaizal, Rozli Zulkifli, Kamaruzaman Sopian, Numerical study of the enhancement of heat transfer for hybrid CuO-Cu nanofluids flowing in a circular pipe, J. Oleo Sci. 62 (7) (2013)533–539.

[50] Abdolreza Moghadassi, Ehsan Ghomi, Fahime Parvizian, A numerical study of water based Al_2O_3 and Al_2O_3–Cu hybrid nanofluid effect on forced convective heat transfer, Int. J. Therm. Sci. 92 (2015) 50–57.
[51] N.A. Usri, W.H. Azmi, Rizalman Mamat, K. Abdul Hamid, G. Najafi, Thermal conductivity enhancement of Al2O3 nanofluid in ethylene glycol and water mixture, Energy Proc. 79 (2015) 397–402.
[52] M.N.F. Mohamad, W.A.W. Hamzah, K.A. Hamid, R. Mamat, Heat transfer performance of Tio2-SiO2 nanofluid in water-ethylene glycol mixture, J. Mech. Eng. 5 (1) (2018) 39–48.
[53] Chandrasekar M, Suresh S, Bose AC. Experimental studies on heat transfer and friction factor characteristics of Al2O3/water nanofluid in a circular pipe under laminar flow with wire coil inserts. Experimental Thermal and Fluid Science. 2010 Feb 1;34(2):122-30.
[54] Hormozi F, ZareNezhad B, Allahyar HR. An experimental investigation on the effects of surfactants on the thermal performance of hybrid nanofluids in helical coil heat exchangers. International communications in heat and mass transfer. 2016 Nov 1;78:271-6.
[55] Barzegarian R, Aloueyan A, Yousefi T. Thermal performance augmentation using water based Al2O3-gamma nanofluid in a horizontal shell and tube heat exchanger under forced circulation. International Communications in Heat and Mass Transfer. 2017 Aug 1;86:52-9.
[56] Wongcharee K, Eiamsa-ard S. Heat transfer enhancement by using CuO/water nanofluid in corrugated tube equipped with twisted tape. International Communications in Heat and Mass Transfer. 2012 Feb 1;39(2):251-7.
[57] Arani AA, Amani J. Experimental study on the effect of TiO2–water nanofluid on heat transfer and pressure drop. Experimental Thermal and Fluid Science. 2012 Oct 1;42:107-15.

ABBREVIATION

MWCNT	:	Multi walled carbon nanotube.
TiO2	:	Titanium dioxide
SWCNT	:	Single walled carbon nanotube
DWCNT	:	Double walled carbon nanotube
DPHE	:	Double pipe heat exchanger
HyNF	:	Hybrid nano fluid
CVD	:	Chemical vapour deposition
SDS	:	Sodium dodecyl sulphate
DI	:	Deionized

TEM	:	Transmission electron microscopy
SEM	:	Scanning electron microscopy
XRD	:	X-ray Diffraction method
DLS	:	Dynamic light scattering.
LMTD	:	Logarithm mean temperature difference.
LPH	:	Liter per hour
HTC	:	Heat transfer Co-efficient.
CFD	:	Computational Fluid Dynamics
C	:	Celsius
m	:	meter
nm	:	Nano meter
Pa	:	Pascal
W	:	Watt
J	:	Joule
K	:	Kelvin
ID	:	Inner diameter
OD	:	Outer diameter
L	:	Length of test section, m
M	:	Mass flow rate kg/s
Q	:	Heat transfer rate, W
C_p	:	Heat capacity, J/kg K
k	:	Thermal conductivity, W/m K
De	:	Equivalent diameter, m
A	:	Cross sectional area, m^2
h	:	Average heat transfer coefficient, $W/m^2.K$
Re	:	Reynolds number
Nu	:	Nusselt number
Pr	:	Prandtl number
T_b	:	Bulk mean temperature, °C
T_{wall}	:	Tube wall temperature, °C
ff	:	Friction factor
p	:	Pressure drop, Pa
g	:	Acceleration due to gravity, m/s2

T_{hi}	:	Temperature of hot inlet, ºC
T_{ho}	:	Temperature of hot outlet, ºC
T_{ci}	:	Temperature of cold inlet, ºC
T_{co}	:	Temperature of cold outlet, ºC

Greek Symbols

ρ	:	Density
Ø	:	Volume fraction
μ	:	Dynamic Viscosity
π	:	pi

Subscripts

i	:	Inlet
o	:	Outlet
f	:	Fluid
W	:	Water
nf	:	Nanofluid
bf	:	Base fluid
avg	:	Average
th	:	Theoretical
exp	:	Experimental
c	:	Cold
h	:	Hot